IEEE Access
Multidisciplinary | Rapid Review | Open Access Journal

Received May 23, 2019, accepted June 11, 2019, date of publication June 27, 2019, date of current version July 19, 2019.

Digital Object Identifier 10.1109/ACCESS.2019.2925417

A Novel Trajectory Planning Method for Automated Vehicles Under Parameter Decision Framework

YUXIANG ZHANG[1], BINGZHAO GAO[1], LULU GUO[2], HONGYAN GUO[2], (Member, IEEE), AND MAOYUAN CUI[3]

[1]State Key Laboratory of Automotive Simulation and Control, Jilin University, Changchun 130022, China
[2]Department of Control Science and Engineering, Jilin University, Changchun 130022, China
[3]China FAW Group Company, Ltd., Changchun 130011, China

Corresponding author: Bingzhao Gao (gaobz@jlu.edu.cn)

This work was supported in part by the National Natural Science Foundation of China under Grant 61520106008, in part by the China Automobile Industry Innovation and Development Joint Fund under Grant U1664257, in part by the State Key Laboratory of Comprehensive Technology on Automobile Vibration and Noise and Safety Control under Grant W65-GNZX-2018-0242, and in part by the Jilin Provincial Science Foundation of China under Grant 20190103047JH.

ABSTRACT Decision and control in all stack scenarios comprise a key issue in the design of automated vehicle control systems. Thus, in higher level, automated vehicles, the decision and the form of the decision should be able to adapt to diverse, changeable, and complex scenarios, which increase the complexity of trajectory planning. In this paper, a parameter decision framework in which the decision is described with key parameters, rather than specific behaviors, such as lane-changing or car-following, is considered. Under this framework, a novel trajectory planning method is proposed to implement behavior with integrated longitudinal and lateral control, in which a nonlinear motion control model is established. The nonlinear model predictive control (NMPC) method with terminal constraints without a predefined path form is applied, which presents more flexibility for changeable decisions. Both the trajectory planning controller and the overall framework are verified by simulation. The results show the validity of the controller and the framework.

INDEX TERMS Model predictive control, trajectory planning, decision-making, integrated longitudinal and lateral control.

I. INTRODUCTION

Automated vehicles, which consist of a hierarchical framework with perception and cognition, decision-making, trajectory planning, and motion control modules, have experienced rapid developments as a result of extensive studies [1]. Except low-cost, high-precision, and high-robustness sensing and perceiving technology, active decision-making and trajectory planning under complex (e.g., intersection navigation or collision avoidance) and changeable (e.g., drivers' intentions suddenly change) traffic scenarios is of vital importance [2]. Under these scenarios, complex decisions are involved. For example, a lane change should involve longitudinal and lateral trajectory planning simultaneously. In the next subsection, the literature on decision-making and trajectory planning is reviewed, and then the original contributions of this paper are discussed.

The associate editor coordinating the review of this manuscript and approving it for publication was Ning Sun.

A. STATE-OF-THE-ART REVIEW AND CHALLENGES

In a hierarchical control framework, the aforementioned subsystems are coordinated and connected by input and output variables. The definition of input and output variables can greatly influence system performance and computational complexity. In decision-making problems, the common method is rule-based and includes scenario-based state machines [3], [4] and Markov decision process models [5], which are predefined by experts [6], [7]. Otherwise, a learning model trained by driving data is used [8], [9]. The decisions in these studies are specific and predefined driving behaviors in a finite set, such as overtaking, lane-maintaining, lane-changing, right-hand turning, etc. [4]. Finite driving behaviors sometimes seems to be conservative or have

This work is licensed under a Creative Commons Attribution 3.0 License. For more information, see http://creativecommons.org/licenses/by/3.0/

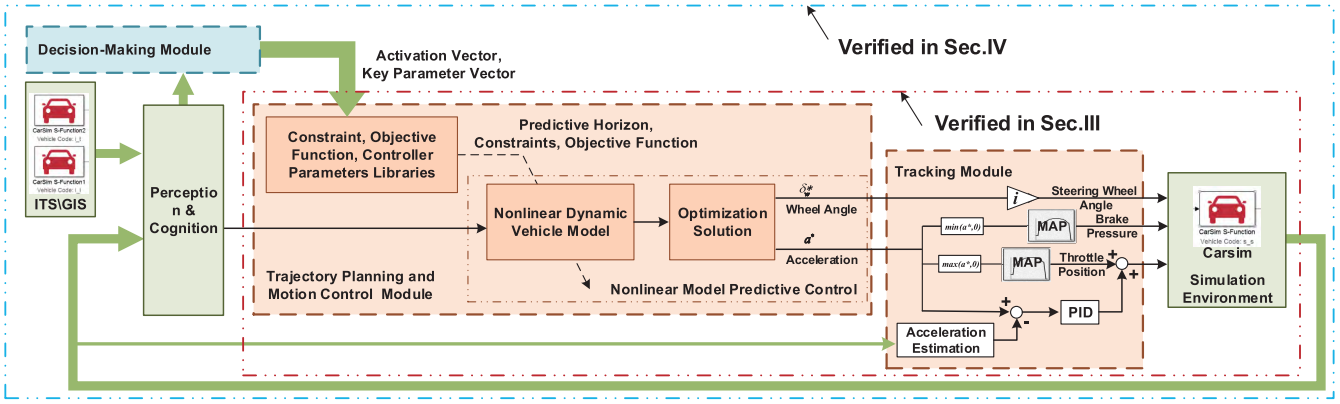

FIGURE 1. Diagram of parameter decision framework.

complicated switch rules to consider more feasible actions. For example, an emergency forward collision condition, despite emergency braking and emergency lane-changing with acceleration or deceleration, can be chosen in some situations [10], [11]. Meanwhile, the great uncertainty and non-linearity of drivers' behaviors can be considered [6]. Moreover, the generalization of driving decisions to non-predefined scenarios should be guaranteed. As illustrated above, the description of a decision could be redefined to cover more complex decisions that can adapt to more scenarios and contain more detailed information about a behavior. In addition, a uniform definition with different decisions can greatly increase the potential for the trajectory planning and motion control module to execute it, even a non-predefined decision in the aforementioned examples. With the consideration that humans react in different scenarios in accordance with specific and bounded physical driving maneuvers, similarly, the complex decisions that are described with corresponding key parameters can cover a wide range of scenarios.

Regarding the trajectory planning methods, current studies mainly contain two kinds of models [12], [13]. Some research tends to consider higher-level planning that considers longitudinal velocity change [14]–[16] while neglecting a vehicle's dynamic characteristics. Other research tends to more heavily consider a vehicle's dynamic characteristics [12], [17], often using a single-track vehicle dynamic model with constant longitudinal velocity [18]. When longitudinal velocity changes are considered, the linear model is transformed into a nonlinear model, which can greatly increase the system complexity. Integrated longitudinal and lateral control is seldom used in trajectory planning [10]. In addition, some research employs predefined trajectory shapes (such as spine curves or polynomial curves [19]–[22]), which are closely related to tasks but lack flexibility when encountering different scenarios and changeable decisions. Furthermore, the scenario-based research illuminates the difference in input and output variables or control forms in the trajectory planning module. For instance, an adaptive cruise-control system involves little lateral control of the vehicle [23], and a lane-changing controller cannot be directly applied to emergency collision avoidance or intersection problems, although lateral control has been involved [12]. Model predictive control (MPC) can be a superior method for the online solution of the optimal trajectory [24], [25]. In MPC methods, the optimal problem can be online solved in a moving predictive horizon [26], [27], which provides great advantages in changing the predictive model, predictive horizon, constraints, performance index, and even the optimal problem form. Different from the current application with MPC-based trajectory planning, firstly, in order to adapt to more scenarios, the model considers more characteristics simultaneously so that it can execute different parameter-based decisions in different scenarios. Secondly, the process of trajectory planning is online solved without a predefined form of trajectory, like a polynomial curve, which brings great advantages to multiple tasks from decisions.

B. WORK AND CONTRIBUTIONS

In this work, under a parameter decision framework, a novel trajectory planning method is proposed to satisfy a wide range of complex scenarios. The main contributions are as follows: 1) To fully represent a wide range of decisions in complex and changeable scenarios, the form of decision is modified with key parameters. 2) Under this kind of decision, the NMPC method is used for trajectory planning because it can generate a trajectory without a fixed form via online solving, and it can also deal with different constraints explicitly. Thus, it can execute various kinds of complex decisions flexibly and react to sudden changes.

The rest of this paper is organized as follows. In Section II, the parameter decision framework is introduced as shown in Fig. 1. Then, the trajectory planning method is described under complex decisions. An integrated trajectory planning and tracking controller is designed, which contains a nonlinear model that considers longitudinal and lateral dynamic characteristics simultaneously. The MPC method is applied with key parameters of the trajectory, rather than a predefined form, which presents more flexibility for changeable decisions. In Section III, verification of the trajectory

planning method is carried out with comparative simulations. In Section IV, the effectiveness of the proposed framework in two complex scenarios is evaluated with parallel simulation in Carsim. The results show the validity of both the framework and controller. Conclusions are given in Section V.

II. PARAMETER DECISION AND TRAJECTORY PLANNING CONTROLLER

In this section, firstly, the parameter decision framework is introduced. Then, the trajectory planning controller, which contains a nonlinear motion control model, is described. The objective function and constraints change with different scenarios and decisions.

A. PARAMETER DECISION FRAMEWORK

Similarly to a common autonomous vehicle control system, the proposed framework is divided into four parts, namely perception and cognition, decision-making, trajectory planning and motion control, and vehicle actuator modules. In this work, we concentrate only on the decision-making, trajectory planning, and motion control modules. That is to say, the perception and cognition and vehicle actuator modules are assumed to be already equipped. In the perception and cognition module, the vehicle perceives the surrounding environment and recognizes other traffic participants. Then, the road information is obtained, such as lane line, velocity limit, and surrounding vehicle movement, including information such as driving direction (straight, opposite direction, right turn, etc.), velocity, and acceleration.

The decision-making module outputs the key parameters about the decision to the trajectory planning and motion control module. The key parameters include behavior's time, lateral displacement, yaw rate, lateral acceleration, and heading angle at terminal state, which varies with different decisions and scenarios. The time, longitudinal velocity change, and terminal position are the most important factors in the decision. Other factors are set to promise a reasonable trajectory after online solving. For example, different terminal constraints are used to plan the trajectory for different road types. Furthermore, the characteristics of the vehicles should be taken into consideration. The scales and rates of control variables are considered to ensure a smooth trajectory. The detailed method will be shown later. As can be seen in the simplified diagram, the planning and control in trajectory calculation are combined without a predefined form, which provides a more flexible framework for trajectory planning and motion control. Meanwhile, at an upper hierarchical level, an optimal problem is established to calculate some parameters of a maneuver that indicates a more complex decision.

B. NONLINEAR MOTION CONTROL MODEL

In the trajectory planning controller, a nonlinear motion control model is used. This model contains a nonlinear vehicle model that considers the longitudinal and lateral dynamics simultaneously as well as a kinematic equation. As the longitudinal dynamic is considered, the single-track vehicle dynamics model is transformed into a nonlinear vehicle model for model predictive control when a changeable longitudinal velocity is considered. The single-track vehicle dynamic model is depicted schematically in Fig. 2. Here, a rear-wheel-driven, front-wheel-steered vehicle is considered. Based on the single-track vehicle dynamics model and a small slip angle β, the dynamic equation can be expressed as

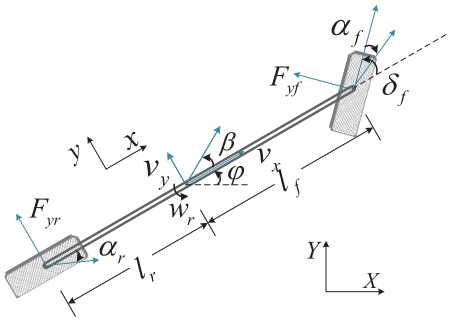

FIGURE 2. Simplified diagram of single-track vehicle dynamic model.

$$M(\dot{v}_y + w_r v_x) = F_{yf} + F_{yr}, \tag{1a}$$
$$I_z \dot{w}_r = l_f F_{yf} - l_r F_{yr}, \tag{1b}$$

where M is the mass of the vehicle, v_x is the longitudinal velocity, v_y is the lateral velocity, w_r is the yaw rate, F_{yf} and F_{yr} are the lateral forces on the front and each rear tires, respectively, I_z is the moment of inertia of the vehicle about the z-axis, and l_f and l_r are the distances from the center of gravity (CoG) to the front and rear axles, respectively. The tire slip angle in the front wheel α_f and rear wheel α_r can be linearized because of the small slip angle, which can be written as

$$\alpha_f = \arctan(\frac{v_y + l_f w_r}{v_x}) - \delta_f \approx \frac{v_y + l_f w_r}{v_x} - \delta_f, \tag{2a}$$
$$\alpha_r = \arctan(\frac{v_y - l_r w_r}{v_x}) \approx \frac{v_y - l_r w_r}{v_x}, \tag{2b}$$

where δ_f is the steering-wheel angle. A concise tire model in the longitudinal velocity change condition is considered, and the lateral tire force can be written as

$$F_{yf} = -C_f \alpha_f = F_{yf}(v_y, w_r, v_x, \delta_f), \tag{3a}$$
$$F_{yr} = -C_r \alpha_r = F_{yr}(v_y, w_r, v_x), \tag{3b}$$

where C_r and C_f are the cornering stiffness values of the front and rear tires, respectively. With the consideration of vehicle kinematics with a geometric relationship in the global coordinate system, the nonlinear motion control model can be established as

$$\dot{x} = f(x, u), \tag{4a}$$

$$f(x,u)=\begin{bmatrix} v_x\cos\varphi - v_y\sin\varphi \\ v_x\sin\varphi + v_y\cos\varphi \\ w_r \\ a \\ \frac{l_f}{I_z}F_{yf} - \frac{l_r}{I_z}F_{yr} \\ \frac{1}{M}F_{yf} + \frac{1}{M}F_{yr} - v_x w_r \end{bmatrix}. \tag{4b}$$

Here, $x = [X, Y, \varphi, v_x, v_y, w_r]$ is the vector of the state; F_{yf}, F_{yr} are the abbreviated forms with Eq. (3), which can be calculated by state variables; $u = [a, \delta_f]$ is the vector of the control variable, a change the longitudinal velocity v_x; φ is the heading angle in the global coordinate system; and X and Y are the coordinates of directions x, y in the global coordinate system. A simple equation about the change of longitudinal velocity v_x is considered and a lower level tracking controller is designed to follow the expected a, which can simplify the motion control model.

C. OBJECTIVE FUNCTION

In this work, an optimal trajectory planning problem is formulated. In the objective function, a smooth trajectory in different decisions is mainly considered. Thus, different indexes can be considered in different decisions, and the indexes can have different levels of importance. These indexes can be control variables u, rate of control variables Δu, lateral velocity v_y, yaw rate w_r, and terminal states such as longitudinal velocity demand v_T or terminal displacement demand X_T, Y_T, which are output by decision-making modules. The aforementioned parameters regarding the decision are denoted as D. These performance indexes are not always necessary, so an activation vector $\mu^o = \{\mu_i^o | i = 1, 2, \ldots, 9\}$ is used, which is determined by the decision-making module. Here, $\mu_i^o \in \{1, 0\}$ represents whether the corresponding equation is adopted or not. In addition, the corresponding weighting factor vector $k = \{k_i | i = 1, 2, \ldots, 9\}$ is selected according to the decision in a weighting factor vector set K. Thus, the objective function can be considered as follows. Given a decision from the decision-making module k, D, μ^o, find $u = [a(t_0), ..., a(t_f), \delta_f(t_0), ..., \delta_f(t_f)]$ such that

$$\begin{aligned} \min J = \int_{t_0}^{t_f} & (\mu_1^o k_1 a(t)^2 + \mu_2^o k_2 \delta_f(t)^2 + \mu_3^o k_3 \Delta a(t)^2 \\ & + \mu_4^o k_4 \Delta\delta_f(t)^2 + \mu_5^o k_5 w_r^2(t) + \mu_6^o k_6 v_y^2(t))dt \\ & + \mu_7^o k_7 (v_x(t_f) - v_T)^2 + \mu_8^o k_8 (X(t_f) - X_T)^2 \\ & + \mu_9^o k_9 (Y(t_f) - Y_T)^2, \end{aligned} \tag{5}$$

where $k_1, k_2, \ldots, k_9$ are the weighting factors in the controller, μ_1^o and $\mu_2^o, \ldots, \mu_9^o$ are corresponding parts in the activation vector, and $v_x(t_f)$, $X(t_f)$, and $Y(t_f)$ are the terminal longitudinal velocity and displacement in the predictive horizon. Here, both integral and terminal performance indexes are considered.

D. INEQUALITY AND EQUALITY CONSTRAINTS

Furthermore, the optimization process must satisfy the constraints, which vary among different scenarios and include both inequality and equality constraints. The constraints in the control variables can be summarized as

$$a_{min} \le a(t) \le a_{max}, \tag{6a}$$
$$\delta_{f,min} \le \delta_f(t) \le \delta_{f,max}, \tag{6b}$$

where $*min$ and $*max$ represent the minimum and maximum bounds, respectively. Since we establish an integrated trajectory planning and tracking controller that contains longitudinal and lateral velocity control simultaneously, the ground attachment constraint in each wheel should be satisfied. To simplify this problem, a_{min} and a_{max} is ± 1.5 when lateral motion control is conducted. Furthermore, the additional road-segment information (e.g., speed limit) can be obtained from the perception and cognition module or from an intelligent transportation system; the constraints of speed can also be added as

$$v_x(t) \le v_{x,max}. \tag{7}$$

Similarly, whether to consider these inequality constraints can also be determined by the decision information from the perception and cognition module, which varies among different scenarios. These constraints can also be activated by $\mu^I = \{\mu_i^I | i = 1, 2, 3\}$.

The equality constraints determine different forms of trajectory, which is of the highest importance in our method. We take straight and curved roads as examples, as shown in Fig. 3. On a straight road, when a vehicle executes a lane-changing decision, a receding predictive horizon problem is applied in which the control horizon is equal to the predictive horizon. Thus, the terminal conditions are given in the following form

$$v_y(t_f) = 0, \tag{8a}$$
$$w_r(t_f) = 0, \tag{8b}$$
$$\varphi(t_f) = 0, \tag{8c}$$
$$y_l(t_f) = y_{l,f}. \tag{8d}$$

Here, y_l is the lateral offset to the centerline of the traffic lane line, and $y_{l,f}$ is the lateral offset between two neighboring

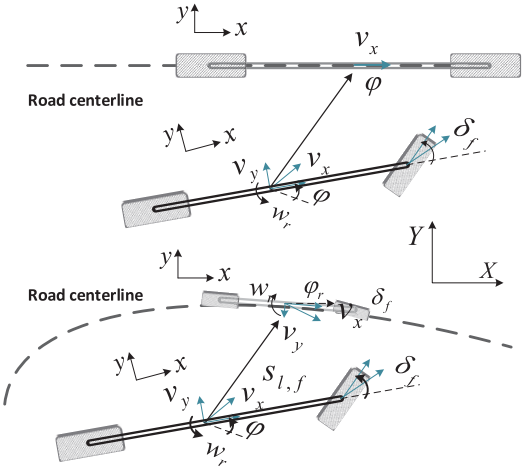

FIGURE 3. Diagram of straight- and curved-road scenarios.

TABLE 1. Sets for objective function, constraints, and parameters.

Objective Function μ^o	μ_1^o	μ_2^o	μ_3^o	μ_4^o	μ_5^o	μ_6^o	μ_7^o	μ_8^o	μ_9^o
Des & Sym	a	δ_f	Δa	$\Delta\delta_f$	w_r	v_y	v_x	X	Y
Type	I	I	I	I	I	I	T	T	T

Constraints μ	μ_1^I	μ_2^I	μ_3^I	μ_1^E	μ_2^E	μ_3^E	μ_4^E	μ_5^E
Des & Sym	Eq.(6a)	Eq.(6b)	Eq.(7)	v_y	w_r	φ	X	y_l
Type	IC	IC	IC	EC	EC	EC	EC	EC

Parameters D	D_1	D_2	D_3	D_4	D_5	D_6	D_7	D_8	D_9
Des & Sym	Mode	Time	$\underline{\mu_7^o}$	$\underline{\mu_8^o}$	$\underline{\mu_9^o}$	$\underline{\mu_3^I}$	$\underline{\mu_3^E}$	$\underline{\mu_4^E}$	$\underline{\mu_5^E}$

* There are two types with objective function (μ_i^o) and two types with constraints (μ_i^I, μ_i^T), in which I and T are the integral and terminal performance indexes, respectively, and IC and EC are the inequality and equality constraints, respectively; the underlined symbols, such as $(\underline{\mu_7^o})$, represent the corresponding expected values.

TABLE 2. Vehicle parameters.

Sym	Des	Value [Unit]
M	vehicle mass	1270 [kg]
I_z	Yaw moment of inertia	1536.7 [kg·m^2]
l_f, l_r	CG distance to front, rear axle	1.015,1.895 [m]
C_f, C_r	Front, rear axle cornering stiffness	1250,755 [N/rad]
u	Attachment coefficient	1
i	Steering ratio	19.7

traffic lane lines. Another common scenario on straight roads is lane-maintaining. In Eq. (8), only Eq. (8d) is changed into

$$y_l(t_f) = 0, \tag{9}$$

and the predictive horizon is held at a fixed length in the lane-maintaining scenario. These terminal equality constraints make the vehicle able to keep its posture on the straight road via online optimization at the end of a predictive horizon.

The lane-changing decision in a curved road-segment is also considered, which may occur in a roundabout or other scenarios. The receding predictive horizon method is adopted as well, and the terminal equality conditions are changed into the following form:

$$\varphi(t_f) = \varphi_r, \tag{10a}$$
$$y_l(t_f) = y_{l,f}. \tag{10b}$$

Here, φ_r is the reference yaw angle that can be transformed by road curvature and vehicle position in the terminal of the predictive horizon with a predictive equation, and the terminal lateral offset $y_{l,f}$ is calculated in the global coordinate system. Similarly, the lane-maintaining decision is transformed with a fixed and shorter predictive horizon. These equality constraints are also activated by $\mu^E = \{\mu_i^E | i = 1, 2, \ldots, 5\}$, and a parameter such as lateral offset $y_{l,f}$ is included in parameter set D.

As illustrated above, the trajectory planning problem in different scenarios can be executed with some simple transformation. The optimal problem can easily change with different activation-function vectors and parameter sets from the decision-making module, which is a more complete description of decisions and is more adaptive to different scenarios.

TABLE 3. Sets for controller evaluation.

P1	P2
$[0, 1, 60, -, -, -, 0, -, 0]$	$[0, 1, 60, -, -, -, 0, -, 0]$
-	$[0, 2, 60, -, -, -, 0, -, 4]$
-	$[0, 1, 60, -, -, -, 0, -, 4]$

P3	P4
$[0, 1, 25, -, -, -, 0, -, 0]$	$[0, 1, 15, -, -, -, 0, -, 0]$
$[1, 3, 25, -, 15, -, \pi/2, -, 15]$	$[1, 2, 15, -, -, -, \pi/2, -, 10]$
$[0, 1, 25, -, -, -, 0, 15, -]$	$[1, 2, 15, -, -, -, \pi, -, 10]$
-	$[0, 1, 15, -, -, -, \pi, -, 10]$

* $\mu^o = [1, 1, 1, 1, 0, 0, 1, 0, 0]$, $\mu^I = [1, 1, 0]$ are same in P1, P2, P3, P4.

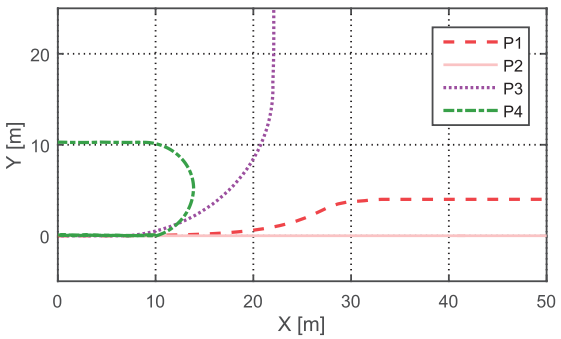

FIGURE 4. Different trajectories in P1, P2, P3, and P4.

To summarize, the items considered in this study are listed in Table 1.

III. TRAJECTORY PLANNING OPTIMIZATION CONTROLLER EVALUATION

In this section, the functionality of the trajectory planning optimization controller is verified with scenarios that are illustrated in Section II. The environment is established in Carsim and jointed with MATLAB/Simulink. Two rear-wheel-drive (RWD) passenger vehicles with internal combustion engines (ICEs) and six-speed automatic transmission are utilized as the environmental vehicles and host vehicle. The vehicle parameters are listed in Table 2. Meanwhile, all the optimal control problems are solved by the optimal toolbox "fmincon" in MATLAB 2015a, wherein the interior point is used.

TABLE 4. Sets for controller evaluation.

Act	μ^E	$T_1 - D$	$T_2 - D$	$T_3 - D$
a	$[1,1,1,0,1]$	$[0,1,60,-,-,-,0,-,-2]$	$[0,1,70,-,-,-,0,-,-2]$	$[0,1,80,-,-,-,0,-,-2]$
A	$[1,1,1,0,1]$	$[1,2.5,65,-,-,-,0,-,2]$	$[1,2.5,65,-,-,-,0,-,2]$	$[1,2.5,72,-,-,-,0,-,2]$
b	$[1,1,1,0,1]$	$[0,1,50,-,-,-,0,-,2]$	$[0,1,40,-,-,-,0,-,2]$	$[0,1,50,-,-,-,0,-,2]$
c	$[0,0,1,0,1]$	$[0,0.5,50,-,-,-,\varphi_r,-,2]$	$[0,0.5,40,-,-,-,\varphi_r,-,2]$	$[0,0.5,50,-,-,-,\varphi_r,-,2]$
B	$[0,0,1,0,1]$	$[1,2.5,45,-,-,-,\varphi_r,-,-2]$	$[1,2.5,45,-,-,-,\varphi_r,-,-2]$	$[1,2.5,45,-,-,-,\varphi_r,-,-2]$
d	$[0,0,1,0,1]$	$[0,0.5,50,-,-,-,\varphi_r,-,-2]$	$[0,0.5,45,-,-,-,\varphi_r,-,-2]$	$[0,0.5,55,-,-,-,\varphi_r,-,-2]$

* $\mu^o = [1,1,1,1,0,0,1,0,0]$, $\mu^I = [1,1,0]$ are same in a, A, b, c, B, d. φ_r is different in each D, which is transformed by road curvature and vehicle position in the terminal of the predictive horizon.

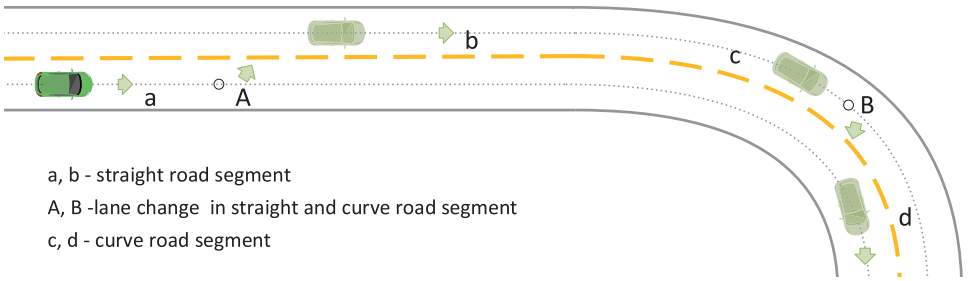

FIGURE 5. Diagram of straight- and curved-road scenarios.

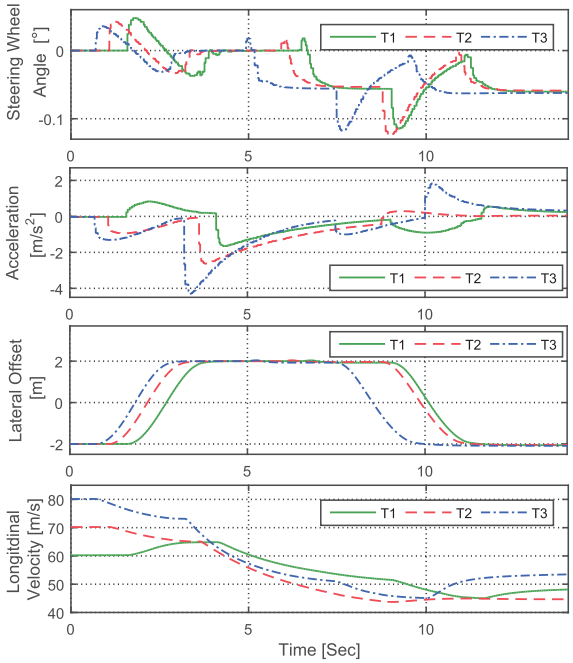

FIGURE 6. Simulation results in controller validation.

First, different trajectories generated with different parameters are implemented to verify the functionality of the trajectory planning optimization controller. The parameters D are shown in Table 3; the results are shown in Fig. 4. This indicates that different trajectories can be generated, such as lane-maintaining (P1), lane-changing (P2), right turning (P3), and turning around (P4).

Secondly, the lane-maintaining and lane-changing maneuvers are implemented on joint straight and curved roads, which are set as shown in Fig. 5. $a, b, c,$ and d are road segments, and A and B are lane-changing maneuvers' points. Before the host vehicle reaches point A, the host vehicle keeps the lane. After the vehicle has changed lanes at point A, a lane-maintaining maneuver is executed as the vehicle travels along the straight and curved road segments until the vehicle reaches point B, then, another curved-road lane change is executed. As we can seen in this process, when the host vehicle approaches the end of the straight road segment, the terminal position is on the curved road in the predictive horizon. Thus, the optimal problem is changed with the position and road type, as with other conditions, which indicates another advantage of this controller. The activation vectors μ^o, μ^I, and μ^E and parameters D in the simulation are shown in Table 4. The foregoing covers decisions such as lane-changing with acceleration and deceleration, lane-maintaining with acceleration and deceleration, and road-form change during lane-maintaining. The planning task changes between lane-changing and lane-maintaining. The optimal problem for trajectory planning under different decisions can be summarized as

$$\begin{aligned}
&\min J = \int_0^{D_2} (k_1 a(t)^2 + k_2 \delta_f(t)^2 + k_3 \Delta a(t)^2 \\
&\qquad +k_4 \Delta \delta_f(t)^2) dt + k_7 (v_x(t_f) - v_T)^2, \\
&s.t.\ \ \dot{x}(t) = f(x(t), u(t), t), \\
&\qquad a_{min} \le a(t) \le a_{max}, \delta_{f,min} \le \delta_f(t) \le \delta_{f,max}, \\
&\qquad \begin{cases} v_y(t_f) = 0, w_r(t_f) = 0, \\ \varphi(t_f) = 0, y_l(t_f) = y_{l,f}. \end{cases} \text{for } P(t_f) \in R_{ac}; \\
&\qquad \varphi(t_f) = \varphi_r, y_l(t_f) = y_{l,f}. \text{for } P(t_f) \in R_{cd}.
\end{aligned} \tag{11}$$

where $P(t_f) = (X(t_f), Y(t_f))$ is the position at the end of predictive horizon. R_{ac} and R_{cd} are the straight and curved road segments, respectively.

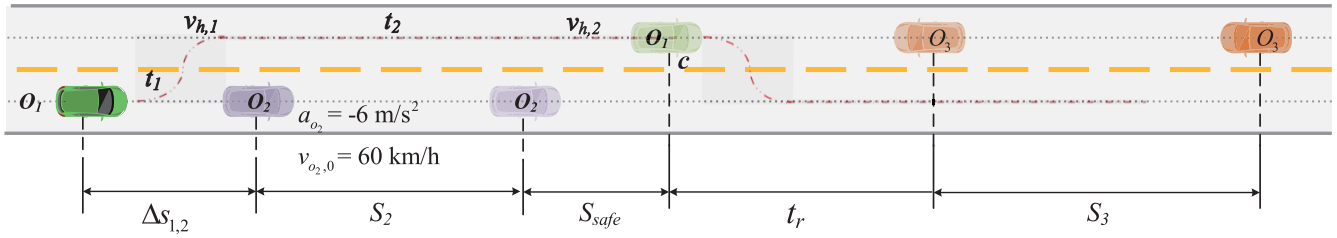

FIGURE 7. Diagram of emergency collision avoidance.

The width of a lane is 4 m, and the radius of the curved-road segment is 50 m. The time for lane-changing is fixed at 2.5s, and the times for straight and curved road segments are 1s and 0.5s, respectively. The simulation results are shown in Fig. 6. To reduce the difficulty of obtaining a solution, the velocity demand is added to the objective function rather than a terminal constraint. Hence, the velocity change in different situations is slightly different because of the optimal solution. Upon making different decisions in different road segments, the trajectory planning optimization controller was demonstrated to be compatible with a wide range of situations, which shows the effectiveness of the trajectory planning controller.

IV. SYSTEM FRAME EVALUATION UNDER COMPLEX SCENARIOS

Two typical scenarios are considered in this section. One is an emergency collision avoidance scenario, and the other is encountering an un-signed intersection, that is, an intersection with no traffic lights, road markings, or signs indicating right-of way. These scenarios have conflict points in the path between the environmental vehicles and host vehicle [28]. The potential conflict is calculated with a prediction method [29]. The intersection area is defined [30]. The rules-based method is applied [31]. Similar problems are usually solved by a time-scheduling problem through conflicts [32]–[35]. Thus, the optimal decision-making problem is established with a time-scheduling problem through conflict points.

A. EMERGENCY COLLISION AVOIDANCE

The diagram of an emergency collision avoidance scenario in a two-way lane is shown in Fig. 7. The preceding vehicle executes emergency braking with a braking deceleration of $-6m/s^2$ from an initial velocity of $60km/h$. The host vehicle follows the preceding vehicle at the same velocity and proper distance. In current autonomous vehicle control systems, the host vehicle will execute emergency braking the same as the preceding vehicle in most cases. In some cases, however, such as a scenario in which there is no vehicle in the oncoming lane or the distance between the oncoming vehicle and host vehicle is sufficiently far, an alternative decision is that the host vehicle takes a collision avoidance path as shown in Fig. 7. The decision varies based on the different running conditions of the oncoming vehicle. Because the oncoming vehicle and host vehicle have a conflict point in the movement point c, such a problem is transformed into a timing problem in that vehicles pass the conflict point with a time difference. If the host vehicle executes an emergency collision avoidance maneuver, the larger time difference can increase safety but may influence passenger comfort in the host vehicle. The remaining time for the vehicle in the oncoming lane to reach the collision point is used to decide the safety level in this scenario. Meanwhile, the lane on the other side of the road is not a common lane for the host vehicle. Thus, if the host vehicle takes a collision avoidance path, the vehicle will first execute a lane change, then overtake the preceding vehicle, and finally return to the previous lane. As we can prove through experiments and analysis, the time of the lane-changing maneuver is the key influencing factor in longitudinal displacement. Considering an emergency scenario, the time of lane change is set as $t_1 = 2.5\ s$, and we choose the velocity of the host vehicle at the end of the lane-change maneuver to be $v_{h,1}$, the time in the oncoming lane to be t_2, and the velocity of the host vehicle before the host vehicle returns to the previous lane to be $v_{h,2}$. Then, the optimal problem is established as follows: Find $u = [v, \triangle v_{h,1}, t_2, \triangle v_{h,2}]$ such that

$$\begin{aligned} \min J = {} & u(1) * (k_{s1,1} t_r + k_{s1,2}(\frac{u(2)}{t_1} + \frac{u(4)}{u(3)})) \\ & + (1 - u(1)) * |a_h|, \\ s.t.\ & t_r > t_{r,min}, v_{h,1} \le v_{max}, v_{h,2} \le v_{max}, \\ & u(3) \ge 0, \triangle v_{min} \le u(2) \le \triangle v_{max}, \end{aligned} \tag{12}$$

where $v_{h,1} = v_{h,0} + \triangle v_{h,1}$ and $v_{h,2} = v_{h,1} + \triangle v_{h,2}$; $v \in \{0, 1\}$ is the decision of whether the host vehicle executes emergency braking or an emergency lane-change maneuver, t_r is the time difference between the two vehicles, which has a limit $t_{r,min}$ to ensure safety, a_h is the brake acceleration of the host vehicle when it chooses to execute emergency braking, and $k_{s1,1}$ and $k_{s1,2}$ are weighting coefficients. Here, the movements of environmental vehicles are just simple predictions in kinematics. The road segment's speed limit is considered as well. Furthermore, the duration in the other lane, t_2, should be positive. Then, the key parameter output by the decision-making module can be expressed as

$$D = \begin{bmatrix} 1 & t_1 & v_{h,1} & 0 & 0 & 80 & 0 & - & 2 \\ 1 & t_2 & v_{h,2} & 0 & 0 & 80 & 0 & d_2 & 2 \\ 1 & t_3 & - & 0 & 0 & 80 & 0 & - & -2 \end{bmatrix}, \tag{13}$$

TABLE 5. Scenario 1 parallel simulation condition.

Scenario Number	P1	P2	P3	P4
O_3 Initial Distance (m)	150	190	230	270
Intention Change	N	Y	Y	N
Acceleration (m/s^2)	0	0.7	0.7	0

* These changed conditions are implemented on vehicle O_3

where $t_1, t_2,$ *and* t_3 are the times of sequential maneuvers, the subscripts correspond to three maneuvers, and $t_1 = t_3$ is the time for lane-changing. Additionally, $d_2 = \Delta s_{1,2} + s_2 + s_{safe}$ is the displacement when the host vehicle returns to the previous lane, $\Delta s_{1,2}$ is the relative displacement between the preceding vehicle and host vehicle, s_2 is the displacement of the preceding vehicle at the end of t_2, and s_{safe} is the safe distance between the two vehicles. Finally, $v_{1,h}$ and $v_{2,h}$ are the expected velocities of the corresponding maneuvers. The activation vector is decided according to the scenario and the decision parameters. This optimal process will continue until the host vehicle has returned to the previous lane, and thus the dimensions of the parameters will decrease.

In simulation, the initial distance between vehicles O_1 and O_3 varies from $150m$ to $270m$. In the initial situation, the vehicles O_1 and O_2 have the same initial velocity of $60km/h$. Then, vehicle O_2 brakes suddenly with a deceleration of $-6m/s^2$. The initial velocity of vehicle O_3 is $40km/h$; it may maintain its velocity, decelerate, or have the intention to accelerate for the reason of not noticing the maneuver of vehicle O_1 or a driver's personalized factor. We have only listed some typical conditions for evaluation in Table 5. Other situations, such as if the vehicle O_3 lowers its velocity or if the initial distance d_3 is large, can be similar to $P4$. The simulation results are shown in Figs. 8, 9, and 10. In these situations, different decisions are implemented. In condition $P1$, as the initial distance is too small, the vehicle O_1 executes emergency braking. In condition $P2$, the vehicle O_3 does not notice the vehicle's overtaking maneuver, so the decision changes after the vehicle O_3 accelerates from overtaking to emergency braking. In condition $P3$, the distance between vehicles O_1 and O_3 is far enough for overtaking; thus, in this process, vehicle O_1 maintains its velocity. In condition $P4$, because of the driver's factor, vehicle O_3 accelerates, but the distance is still sufficient for overtaking. To ensure safety, vehicle O_1 accelerates as well. As can be seen in Fig. 10, the colored areas represent the situations in which vehicles O_1 and O_2 or O_1 and O_3 are in the same lane. Vehicle O_2 is in the right-hand lane, whose lateral offset is -2, and vehicle O_3 is in the left-hand lane, whose lateral offset is 2. When the lateral offset of vehicle O_1 is less than -0.5, it is assumed to be in the right-hand lane. When the lateral offset of the same vehicle is greater than 0.5, it is assumed to be in the left-hand lane. Simulation shows that in the optimization of decision-making, the safety criterion is satisfied with changeable decisions with a uniform trajectory planning controller.

B. UN-SIGNED INTERSECTION

The host vehicle makes a left-turn maneuver when there are some other vehicles in other lanes. In this situation,

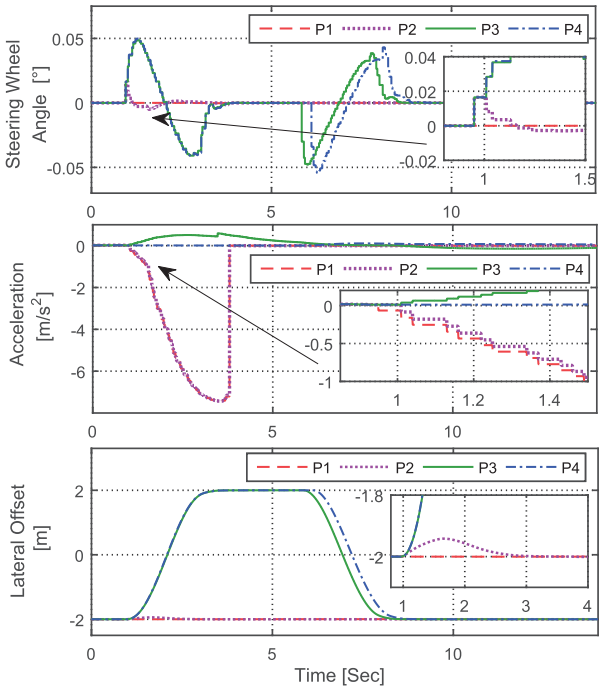

FIGURE 8. Steering angle, acceleration, and lateral offset in different conditions.

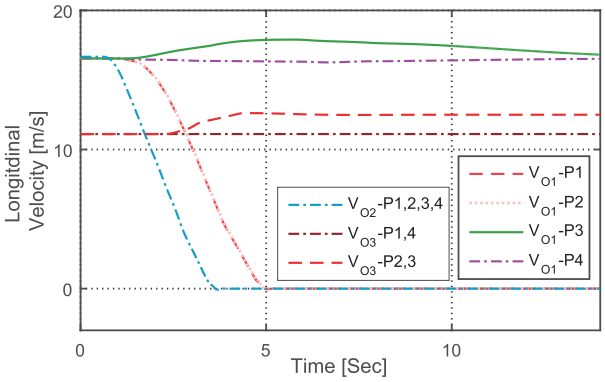

FIGURE 9. Velocity profiles of vehicles O_1, O_2, O_3 in different conditions.

three conflict points are taken into consideration. To avoid collision, the timing sequence to the collision points should be managed. The relevant simplified diagram is depicted in Fig. 11, in which two lanes are drawn when in actuality there are four lanes in each direction. It should be emphasized that this method should only be applied in the situation in which there are more than three lanes in each direction, because it is more suitable for the intersection scenario to be simplified as a timing problem when the number of lanes is less than three. The vehicles $O_1, O_2,$ and O_3 are the vehicles in these lanes. The expression $oo = [oo_1, oo_2, oo_3]$ where $oo_i \in \{0, 1\}$ represents the situation in which there is a vehicle in each lane or not. Three conflict points are taken into consideration as possible constraint points. Thus, the times to these points are control variables. When there is no vehicle in the lane or there are none in the oncoming

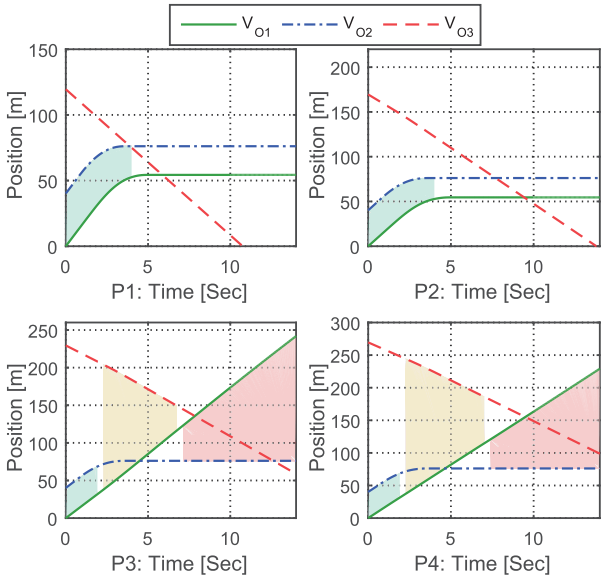

FIGURE 10. Longitudinal displacement of vehicles O_1, O_2, and O_3 in different conditions. The light-green-colored area represents vehicles O_1 and O_2 both being in the right-hand lane, the light-yellow-colored area represents vehicles O_1 and O_3 both being in the left-hand lane, and the light-red-colored area represents vehicles O_1 and O_2 both being in the right-hand lane.

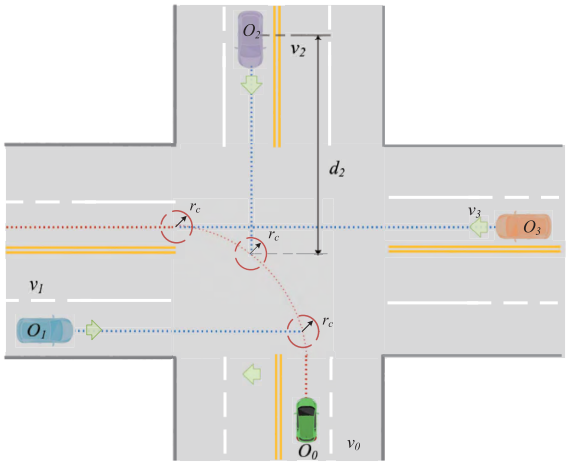

FIGURE 11. Diagram of crossroads with no traffic lights.

direction, the corresponding control variables are neglected. The position of the host vehicle is calculated and represented as $op = [op_1, op_2, op_3]$, where $op_i \in \{0, 1\}$ represents whether the host vehicle has passed the corresponding point. Thus, the dimension of control variables is $n = sum(oo \cdot op)$. Taking $\boldsymbol{n}$= 3 as an example, the decision problem is established as follows: Find $u = [t_{h,1}, t_{h,2}, t_{h,3}]$ such that

$$\min J = k_{s2,1} \cdot \sum_{i=1}^{3} u(i) + k_{s2,2} \cdot \sum_{i=1}^{3} \left(\frac{s_{i-1}}{s} \cdot \sum_{i=1}^{3} u(i) - u(i)\right)^2 + k_{s2,3} \cdot \left(\frac{s}{v_h} - \sum_{i=1}^{3} u(i)\right)^2 + k_{s2,4} \cdot \left(\frac{s}{v_r} - \sum_{i=1}^{3} u(i)\right)^2,$$

$$s.t. \quad \left(\sum_{j=1}^{i} u(j) - t_{\overline{oi}}\right)\left(\sum_{j=1}^{i} u(j) - t_{\underline{oi}}\right) \geq 0, \quad u(i) \geq 0, i = 1, 2, 3, \tag{14}$$

where $t_{h,1}$, $t_{h,2}$, and $t_{h,3}$ are time intervals between the three conflict points. Because there is no centerline in the area of the intersection, the original reference centerline (straight road) is defined to calculate the distance $s_i (i = 1, 2, 3)$ between these phases, and $s = \sum_{i=1}^{3} s_i$; v_h is the current velocity of the host vehicle; v_r is the expected velocity in the intersection; and $k_{s2,1}$, $k_{s2,2}$, $k_{s2,3}$, and $k_{s2,4}$ are the weights of each performance index. The objective function considers the total time, time distribution, and comfort. The variables $t_{\underline{o1}}$, $t_{\overline{o1}}$, $t_{\underline{o2}}$, $t_{\overline{o2}}$, $t_{\underline{o3}}$, and $t_{\overline{o3}}$ are the time intervals for vehicles O_1, O_2, and O_3 to reach and leave the conflict point in the path for the host vehicle. These constraints are set to ensure safety. When $t_{h,1} > t_{\overline{o1}}$, the oncoming vehicle will pass the collision point first. Otherwise, the host will pass the intersection before the oncoming vehicle. As turning is a continuous behavior, the decision is merged when the decision indicates that there is no interaction in the phase of behavior. Thus, when there is no stopping and another conflict point should be considered, the parameter D about the merged decision can be expressed as

$$D = \left[1 \sum_{i=1}^{3} u(i) - - L_0\ 45\ \pi/2\ L_0 - \right], \tag{15}$$

where $L_0 = 9/16 \cdot L$, $L = 32$ is the length of the square crossroad area.

TABLE 6. Scenario 2 parallel simulation condition.

Scenario Number	S2-1	S2-2	S2-3
Ini Dis (m)	120,90,100	60,100,70	70,65,100
Ini Spd (km/h)	25,20,20	30,25,20	20,25,25
If IC/T (s)	N	N	Y/1.5

*Respective conditions of O_1, O_2, and O_3 are shown. Ini Dis is the initial distance. Ini Spd is the initial speed. If IC/T means whether the intention changes or not and the intention change time

In the right-turn intersection scenario, the sets of parallel simulation conditions are listed and labeled in Table 6. Similarly, the steering angle and acceleration in Scenario 2 with different conditions are shown in Fig. 12. In condition S2-1, the vehicles O_1, O_2, and O_3 are sufficiently far from the intersection. Therefore, the host vehicle O_0 decelerates first and then maintains its speed when in the intersection. In condition S2-2, the distance of vehicle O_0 is just beyond distance of vehicle O_1 to the intersection. Therefore, vehicle O_0 maintains its speed and even slightly accelerates to ensure safety with the intention of driving through the intersection in front of vehicle O_3. In condition S2-3, vehicle O_0 decelerates when approaching the intersection. Vehicle O_2 has the intention of accelerating at 1.5 s, and vehicle O_0 accelerates because vehicle O_0 is closer to the intersection. The paths of the three conditions are shown in the upper left of Fig. 13. The remaining time to reach each conflict point of these vehicles is calculated to show the time series. The colored

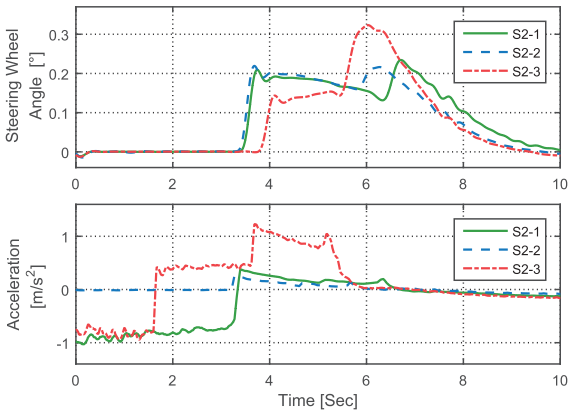

FIGURE 12. Steering angle and acceleration in Scenario 2 with different conditions.

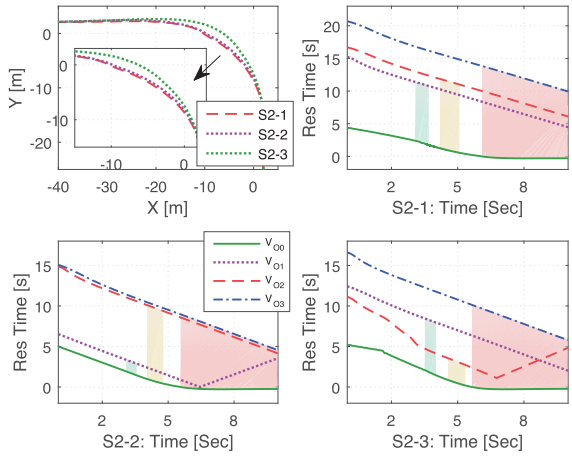

FIGURE 13. Trajectory of vehicle O_0 in different conditions is shown at upper left. Remaining times of vehicles O_0, O_1, O_2, and O_3 to reach the conflict points in different conditions are shown in the other three subplots. The light-green-, light-yellow and light-red-colored area in each subplot represents vehicles O_0 and O_1 being in one lane, vehicles O_0 and O_2 being in one lane, and vehicles O_0 and O_3 being in one lane.

areas represent that two vehicles are in the same lane. Simulation shows that the trajectory planner can calculate the optimal trajectory in different scenarios and conditions, which indicates that it can adapt to more complex and changeable decisions.

V. CONCLUSIONS

In this paper, to expand the adaptive range of automated vehicles in multiple scenarios, a novel trajectory planning method under a parameter decision framework is proposed. The decision behavior is represented by several key parameters that are related to trajectory and can be applied to the trajectory planning and motion control module in multiple scenarios. The MPC method, with a nonlinear motion model and terminal constraints, is applied, which can plan longitudinal and lateral trajectory via online solving. The effectiveness of the trajectory planning method is verified by comparative simulations. In addition, the overall framework is tested in two complex scenarios with parallel simulation. Results show the validity of both the framework and controller.

In future works, an automated method of devising a scenario and forming an optimal decision-making problem will be explored. Machine-learning methods will mainly be considered in the development of this automated method. Furthermore, the automated vehicle behavior in a multi-agent environment in which agents behave interactively will be studied. The behavior of other vehicles should be considered as well. Finally, the vehicle model in this paper considered only a simple tire model. More complex tire models should be considered in the future, which will increase the difficulty of solving the optimal problem. Thus, fast-solving algorithms should also be investigated.

REFERENCES

[1] B. Paden, M. Čáp, S. Z. Yong, D. Yershov, and E. Frazzoli, "A survey of motion planning and control techniques for self-driving urban vehicles," *IEEE Trans. Intell. Veh.*, vol. 1, no. 1, pp. 33–55, Mar. 2016.

[2] A. Li, W. Zhao, S. Li, X. Qiu, and X. Wang, "Research on the motion trajectory optimization method based on the improved genetic algorithm for an intelligent vehicle," *Proc. Inst. Mech. Eng. D, J. Automobile Eng.*, vol. 230, no. 13, pp. 1729–1740, 2016.

[3] S. Noh and K. An, "Decision-making framework for automated driving in highway environments," *IEEE Trans. Intell. Transp. Syst.*, vol. 19, no. 1, pp. 58–71, Jan. 2018.

[4] C. Guo, K. Kidono, R. Terashima, and Y. Kojima, "Toward human-like behavior generation in urban environment based on Markov decision process with hybrid potential maps," in *Proc. IEEE Intell. Vehicles Symp. (IV)*, Jun. 2018, pp. 2209–2215.

[5] E. Sonu, Z. Sunberg, and M. J. Kochenderfer, "Exploiting hierarchy for scalable decision making in autonomous driving," in *Proc. IEEE Intell. Vehicles Symp. (IV)*, Jun. 2018, pp. 2203–2208.

[6] Z. Li, B. Wang, J. Gong, T. Gao, C. Lu, and G. Wang, "Development and evaluation of two learning-based personalized driver models for pure pursuit path-tracking behaviors," in *Proc. IEEE Intell. Vehicles Symp. (IV)*, Jun. 2018, pp. 79–84.

[7] C. Hubmann, J. Schulz, M. Becker, D. Althoff, and C. Stiller, "Automated driving in uncertain environments: Planning with interaction and uncertain maneuver prediction," *IEEE Trans. Intell. Vehicles*, vol. 3, no. 1, pp. 5–17, Mar. 2018.

[8] L. Chong, M. M. Abbas, A. M. Flintsch, and B. Higgs, "A rule-based neural network approach to model driver naturalistic behavior in traffic," *Transp. Res. C, Emerg. Technol.*, vol. 32, pp. 207–223, Jul. 2013.

[9] C. Vallon, Z. Ercan, A. Carvalho, and F. Borrelli, "A machine learning approach for personalized autonomous lane change initiation and control," in *Proc. IEEE Intell. Vehicles Symp. (IV)*, Jun. 2017, pp. 1590–1595.

[10] A. Arikere, D. Yang, M. Klomp, and M. Lidberg, "Integrated evasive manoeuvre assist for collision mitigation with oncoming vehicles," *Vehicle Syst. Dyn.*, vol. 56, no. 10, pp. 1577–1603, 2018.

[11] H. Cao, X. Song, Z. Huang, and L. Pan, "Simulation research on emergency path planning of an active collision avoidance system combined with longitudinal control for an autonomous vehicle," *Proc. Inst. Mech. Eng., Part D, J. Automobile Eng.*, vol. 230, no. 12, pp. 1624–1653, 2016.

[12] K. Liu, J. Gong, A. Kurt, H. Chen, and U. Ozguner, "Dynamic modeling and control of high-speed automated vehicles for lane change maneuver," *IEEE Trans. Intell. Veh.*, vol. 3, no. 3, pp. 329–339, Sep. 2018.

[13] J. Kong, M. Pfeiffer, G. Schildbach, and F. Borrelli, "Kinematic and dynamic vehicle models for autonomous driving control design," in *Proc. IEEE Intell. Vehicles Symp. (IV)*, Jun./Jul. 2015, pp. 1094–1099.

[14] J. Wei, J. M. Snider, T. Gu, J. M. Dolan, and B. Litkouhi, "A behavioral planning framework for autonomous driving," in *Proc. IEEE Intell. Vehicles Symp.*, Jun. 2014, pp. 458–464.

[15] C. Liu, S. Lee, S. Varnhagen, and H. E. Tseng, "Path planning for autonomous vehicles using model predictive control," in *Proc. IEEE Intell. Vehicles Symp. (IV)*, Jun. 2017, pp. 174–179.

[16] D. González, J. Pérez, V. Milanés, and F. Nashashibi, "A review of motion planning techniques for automated vehicles," *IEEE Trans. Intell. Transp. Syst.*, vol. 17, no. 4, pp. 1135–1145, Apr. 2016.

[17] J. Ji, A. Khajepour, W. W. Melek, and Y. Huang, "Path planning and tracking for vehicle collision avoidance based on model predictive control with multiconstraints," *IEEE Trans. Ultrason. Eng.*, vol. 66, no. 2, pp. 952–964, Feb. 2017.
[18] J. Guo, Y. Luo, K. Li, and Y. Dai, "Coordinated path-following and direct yaw-moment control of autonomous electric vehicles with sideslip angle estimation," *Mech. Syst. Signal Process.*, vol. 105, pp. 183–199, May 2018.
[19] M. Saska, V. Spurný, and V. Vonásek, "Predictive control and stabilization of nonholonomic formations with integrated spline-path planning," *Robot. Auton. Syst.*, vol. 75, pp. 379–397, Jan. 2016.
[20] X. Li, Z. Sun, D. Cao, Z. He, and Q. Zhu, "Real-time trajectory planning for autonomous urban driving: Framework, algorithms, and verifications," *IEEE/ASME Trans. Mechatronics*, vol. 21, no. 2, pp. 740–753, Apr. 2016.
[21] H. Guo, C. Shen, H. Zhang, H. Chen, and R. Jia, "Simultaneous trajectory planning and tracking using an MPC method for cyber-physical systems: A case study of obstacle avoidance for an intelligent vehicle," *IEEE Trans. Ind. Informat.*, vol. 14, no. 9, pp. 4273–4283, Sep. 2018.
[22] Z. Feng, S. Chen, Y. Chen, and N. Zheng, "Model-based decision making with imagination for autonomous parking," in *Proc. IEEE Intell. Vehicles Symp. (IV)*, Jun. 2018, pp. 2216–2223.
[23] A. Vahidi and A. Eskandarian, "Research advances in intelligent collision avoidance and adaptive cruise control," *IEEE Trans. Intell. Transp. Syst.*, vol. 4, no. 3, pp. 143–153, Sep. 2003.
[24] H. Guo, F. Liu, R. Yu, Z. Sun, and H. Chen, "Regional path moving horizon tracking controller design for autonomous ground vehicles," *Sci. China Inf. Sci.*, vol. 60, no. 1, 2017, Art. no. 013201.
[25] Q. Cui, R. Ding, B. Zhou, and X. Wu, "Path-tracking of an autonomous vehicle via model predictive control and nonlinear filtering," *Proc. Inst. Mech. Eng. D, J. Automobile Eng.*, vol. 232, no. 9, pp. 1237–1252, 2018.
[26] X. Gong, I. Kolmanovsky, E. Garone, K. Zaseck, H. Chen, "Constrained control of free piston engine generator based on implicit reference governor," *Sci. China Inf. Sci.*, vol. 61, no. 7, p. 70203, Jul. 2018.
[27] H. Guo, D. Cao, H. Chen, Z. Sun, and Y. Hu, "Model predictive path following control for autonomous cars considering a measurable disturbance: Implementation, testing, and verification," *Mech. Syst. Signal Process.*, vol. 118, pp. 41–60, Mar. 2019.
[28] J. Nilsson, M. Brännström, J. Fredriksson, and E. Coelingh, "Longitudinal and lateral control for automated yielding maneuvers," *IEEE Trans. Intell. Transp. Syst.*, vol. 17, no. 5, pp. 1404–1414, May 2016.
[29] W. Song, G. Xiong, and H. Chen, "Intention-aware autonomous driving decision-making in an uncontrolled intersection," *Math. Problems Eng.*, vol. 2016, Mar. 2016, Art. no. 1025349.
[30] Y. Liu and U. Ozguner, "Human driver model and driver decision making for intersection driving," in *Proc. IEEE Intell. Vehicles Symp.*, Jun. 2007, pp. 642–647.
[31] M. Hülsen, J. M. Zöllner, and C. Weiss, "Traffic intersection situation description ontology for advanced driver assistance," in *Proc. IEEE Intell. Vehicles Symp. (IV)*, Jun. 2011, pp. 993–999.
[32] G. R. de Campos, P. Falcone, R. Hult, H. Wymeersch, and J. Sjöberg, "Traffic coordination at road intersections: Autonomous decision-making algorithms using model-based heuristics," *IEEE Intell. Transp. Syst. Mag.*, vol. 9, no. 1, pp. 8–21, 2017.
[33] H. Ahn, A. Colombo, and D. D. Vecchio, "Supervisory control for intersection collision avoidance in the presence of uncontrolled vehicles," in *Proc. Amer. Control Conf.*, Jun. 2014, pp. 867–873.
[34] A. Colombo and D. D. Vecchio, "Least restrictive supervisors for intersection collision avoidance: A scheduling approach," *IEEE Trans. Autom. Control*, vol. 60, no. 6, pp. 1515–1527, Jun. 2015.
[35] H. Ahn and D. D. Vecchio, "Safety verification and control for collision avoidance at road intersections," *IEEE Trans. Autom. Control*, vol. 63, no. 3, pp. 630–642, Mar. 2018.

YUXIANG ZHANG received the B.S. and Ph.D. degrees in vehicle engineering and control theory and engineering from Jilin University, Changchun, China, in 2014 and 2019, respectively.

Her current research interests include advanced vehicle powertrain control, energy management of hybrid electric vehicles, and cybersecurity of connected vehicles.

BINGZHAO GAO received the B.S. degree from the Jilin University of Technology, China, in 1998, the M.S. degree from Jilin University, China, in 2002, and the Ph.D. degrees in mechanical engineering from Yokohama National University, Japan, and in control engineering from Jilin University, in 2009. He is currently a Professor with Jilin University. His research interests include vehicle powertrain control and vehicle stability control.

LULU GUO received the B.S. and Ph.D. degrees in vehicle engineering and control theory and engineering from Jilin University, Changchun, China, in 2014 and 2019, respectively.

His current research interests include advanced vehicle powertrain control, energy management of hybrid electric vehicles, and cybersecurity of connected vehicles.

HONGYAN GUO (M'17) received the Ph.D. degree in control theory and control engineering from Jilin University, Changchun, China, in 2010.

She joined Jilin University, in 2011, where she has been an Associate Professor, since 2014, and has been a Professor with the Department of Control Science and Engineering, since 2018. Since 2017, she has also been a Visiting Scholar with Cranfield University, Cranfield, U.K. Her current research interests include path tracking, and stability control of autonomous vehicles and vehicle states estimation.

MAOYUAN CUI was born in Liaoning, China. He received the Ph.D. degree in control theory and control engineering from Jilin University, Changchun, China, in 2004. His current research interests include autonomous vehicle system design, sensor fusion, localization, path planning, and motion control.